Evaluation of Hot Cracking in Nitrogen-Bearing and Fully Austenitic Stainless Steel Weldments

Nitrogen increases fusion zone and HAZ cracking in stainless steel

BY V. SHANKAR, T. P. S. GILL, S. L. MANNAN AND S. SUNDARESAN

ABSTRACT. Stainless steels exhibiting a primary austenitic solidification mode are particularly susceptible to hot cracking during welding. It is often difficult to predict the behavior of such materials, since the cracking is extremely sensitive to levels of impurity and minor elements such as P, S and N. In this work, the fusion zone and HAZ cracking behavior of a nitrogen-bearing AISI Type 316LN steel and fully austenitic Alloy D9 were investigated using the Varestraint Test. The results of the cracking tests were compared with that of a conventional primary ferritic 316L composition. The crack length measurements revealed that the 316LN was highly susceptible to fusion zone and HAZ cracking, while Alloy D9 was moderately susceptible. Analysis of the cracking data revealed that the total crack length criterion provided a better estimate of weldability than maximum crack length and brittleness temperature range criteria. Correlation of the composition and cracking susceptibility — including data obtained from the literature — indicated an interaction between nitrogen and phosphorus in enhancing cracking. A high degree of base and weld metal HAZ microfissuring was produced in 316LN, in comparison with 316L, which was attributed to the detrimental effect of nitrogen in this alloy. Heat-affected zone cracks were quite susceptible to backfilling, presumably due to favorable capillary and thermal conditions in this region.

Introduction

Hot cracking is an important problem encountered during the welding of austenitic stainless steels (Refs.1, 2). It is established that hot cracking occurs by the formation of low-melting eutectic phases in the solidifying weld metal and in the heat-affected zone (HAZ), under the action of shrinkage stresses and restraint imposed on the joint (Refs.1–3). In the HAZ, cracking occurs by liquation of grain boundaries in the partially melted zone adjacent to the fusion line and in previously deposited weld metal in a multipass weld (Ref. 4). It has been found that cracking can be greatly reduced by selecting compositions that solidify in the ferritic mode (Ref. 5), or by reducing the concentration of impurity elements such as P, S, etc., to very low levels (Refs. 6, 7). However, in the case of some materials, such as fully austenitic stainless steels and nitrogen-bearing stainless steels, a primary ferritic solidification mode may not occur. In such cases, the levels of impurity and minor elements may critically determine the cracking behavior.

In this work, the weld metal and HAZ cracking behavior of one nitrogen-bearing AISI 316LN and a fully austenitic Ti-stabilized 15Cr-15Ni-2Mo stainless steel D9 (corresponding to ASTM A-771/ UNS S38660) has been determined. The nitrogen-bearing stainless steels have gained importance because of their superior high-temperature properties and resistance to sensitization over conventional AISI 316L. The fully austenitic D9 alloy has been developed (Ref. 8) for use in core components of fast-breeder reactors because of its resistance to irradiation damage. These materials are candidates for use in the Indian fast-breeder reactor program and it was essential to assess accurately their hot cracking susceptibility. A conventional Type 316L composition was also tested for comparison.

KEY WORDS

Austenitic
Stainless Steel
Weldability
Hot Cracking
HAZ Cracking
GTAW

The addition of nitrogen is known to have a strong effect on weld microstructures (Refs. 9–14). The delta-ferrite content decreases and the solidification mode changes from primary ferritic to primary austenitic. Several studies have also been carried out on the effect of nitrogen on the cracking susceptibility of stainless steels. Matsuda, *et al.* (Ref. 12), found that in Type 304 weld metals, nitrogen addition increased the brittleness temperature range (BTR) to levels obtained in fully austenitic 310 material even when 1–3% delta-ferrite was present in the microstructure. They found enhanced phosphorus segregation with an increase in nitrogen content. However, in primary austenitic 316L (Refs. 9, 14), it has been found that nitrogen actually reduces cracking, accompanied by a refinement in solidification substructure. Nitrogen is also known to promote cracking in the weld metal HAZ (Refs. 15, 16), at locations where transformation of the delta-ferrite in the underlying weld bead takes place. Despite the various studies available on cracking in nitrogen-bearing stainless steels, comprehensive information on hot cracking susceptibility is lacking.

In fully austenitic materials, the tolerable impurity levels for good weldability are generally low (Refs. 6, 7). Moreover, in Alloy D9, the presence of titanium increases the likelihood of liquation cracking in the HAZ. Titanium is known to promote HAZ cracking in A286 and in Alloy 800 (Refs. 17, 18) and desirable levels of titanium depend on the carbon content. Titanium in excess of a Ti/C ratio of 5 is considered detrimental (Ref. 19). On the other hand, certain minimum levels of elements such as Ti and P are desirable for irradiation swelling resistance (Ref. 8). Hence, the composition of such a material must be optimized for good weldability. As information on the weldability of Alloy D9 is scarce, it was nec-

V. SHANKAR, T. P. S. GILL and S. L. MANNAN are with the Materials Development Division, Indira Gandhi Centre for Atomic Research, Kalpakkam, India. S. SUNDARESAN is with the Department of Metallurgical Engineering, Indian Institute of Technology, Madras, India.

Table 1 — Chemical Compositions of the Materials Tested

	C	Ni	Cr	Mo	Mn	Si	P	S	N	Other
316L	0.029	11.90	17.0	2.25	1.80	0.70	0.035	0.012	0.036	—
316LN	0.030	11.15	16.8	2.06	1.45	0.53	0.031	0.001	0.073	—
Alloy D9	0.052	15.06	15.05	2.25	1.50	0.50	0.011	0.002	0.066	0.33 Ti

Table 2 — Welding Parameters used for Varestraint Testing

Current	100 A
Voltage	10 V
Travel Speed	4.2 mm/s
Argon Flow Rate	141/min
Diameter of W — Electrode	2.4 mm
Electrode Tip Angle	60°
Arc Gap	1.6 mm

essary to evaluate its cracking behavior.

In this study, a 3-bead moving torch Varestraint Test technique proposed by Lundin (Refs. 19, 20) has been used to simultaneously reveal cracking in the weld metal as well as the base and weld metal HAZs.

Experimental Procedures

Materials

Three materials, namely AISI Types 316L and 316LN and Alloy D9, were studied in this work. Their chemical compositions are given in Table 1. The 316LN contains a controlled nitrogen addition of 0.06–0.08%, while D9 is a 15Cr-15Ni-2Mo fully austenitic steel containing 0.33% titanium. The 316L and 316LN alloys in their as-received mill annealed condition were 3.15 mm and 2.85 mm in thickness, while the D9 material was forged from rod stock, rolled down to 3.15 mm sheet and solution-annealed prior to testing.

Hot Cracking Tests

Hot cracking susceptibility of the materials was tested on a Moving Torch Varestraint Hot Cracking Test Device, Model LT1100. The equipment consists of a torch movement assembly and a pneumatic straining assembly. The equipment and test configuration are shown in Fig. 1 (Refs. 14, 19). As shown in Fig. 1, the test subjects a GTA weld deposited on the specimen to a controlled strain application. The specimen is constrained horizontally and vertically at the ends, except for axial sliding, and welding is started at one end. The strain is suddenly applied so as to "freeze" the position of the solid-liquid interface. The strain application produces cracking in the vicinity of this interface, the extent of which depends on the material's susceptibility. Varestraint Test specimens of dimensions 125 x 25 x 3 mm were prepared with the length along the rolling direction. The 3-bead longitudinal Varestraint Test procedure used by Lundin and coworkers (Refs. 14, 19, 20) was used in the present work. Two weld passes were made with a separation of 5–6 mm without applying strain. The welding parameters (given in Table 2) were chosen such that a penetration of slightly more than 50% of the specimen thickness was achieved with a bead width of 4–5 mm. The strain was applied during the third pass, which was made so as to overlap one of the earlier ones, as shown in Fig. 1. The second pass was essentially applied to balance the thermal contractions along the width direction about the longitudinal axis of the specimen (Ref. 14). This technique enabled simultaneous study of HAZ cracking in the base metal heat-affected zone (BMHAZ), the weld metal heat-affected zone (WMHAZ) and fusion zone cracking.

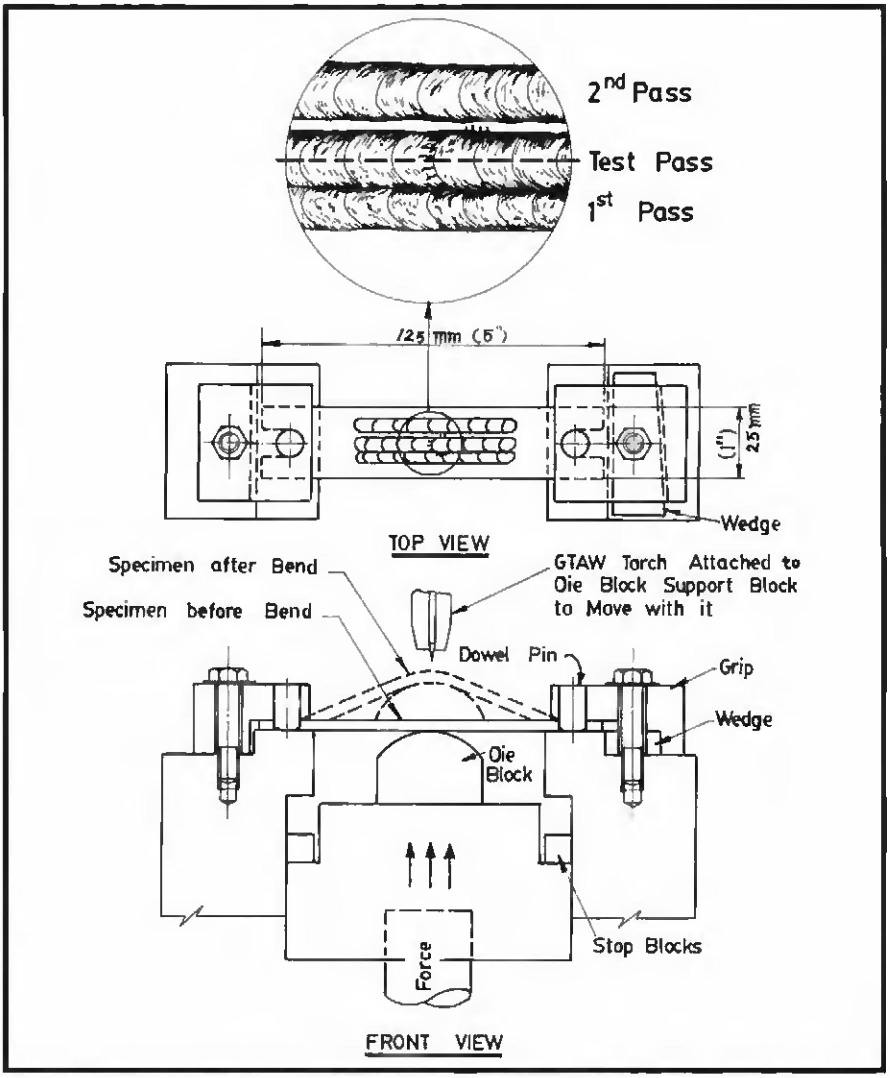

Fig. 1 — Schematic diagram of the Varestraint Test equipment showing the test procedure and location of cracking.

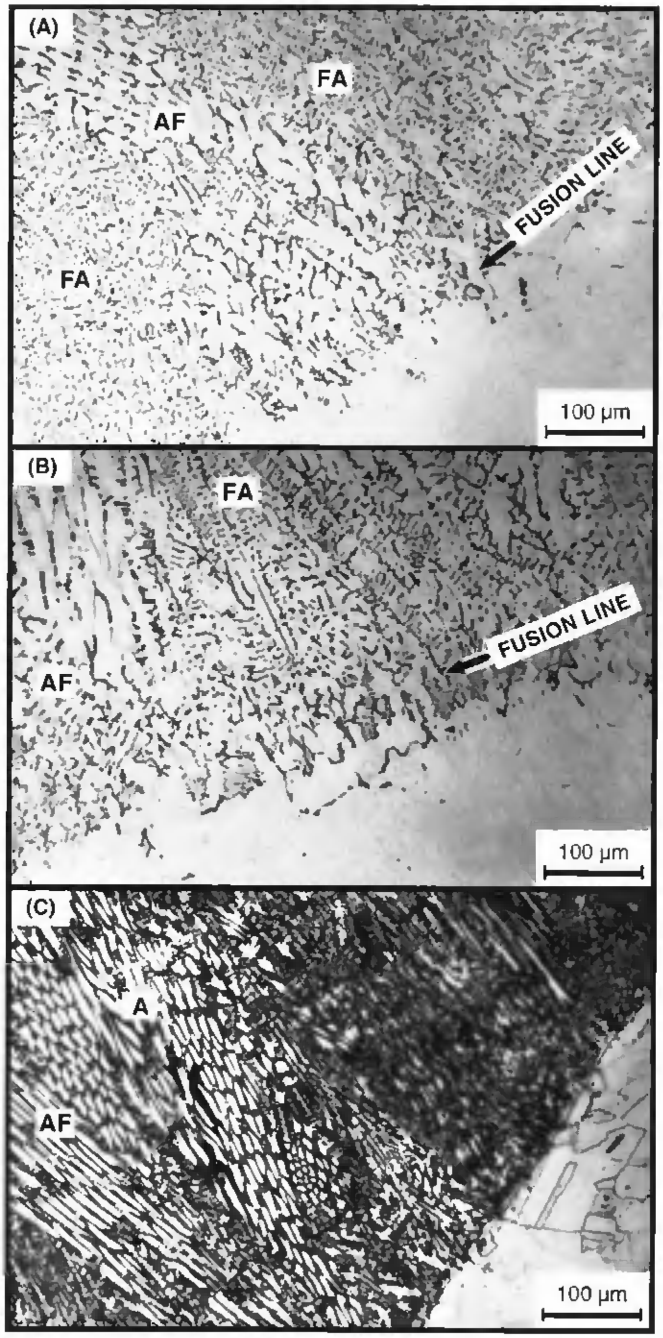

Fig. 2 — Weld microstructures of stainless steels 316L, 316LN and Alloy D9 showing solidification mode and ferrite morphology in: A — 316L; B — 316LN; and C — Alloy D9.

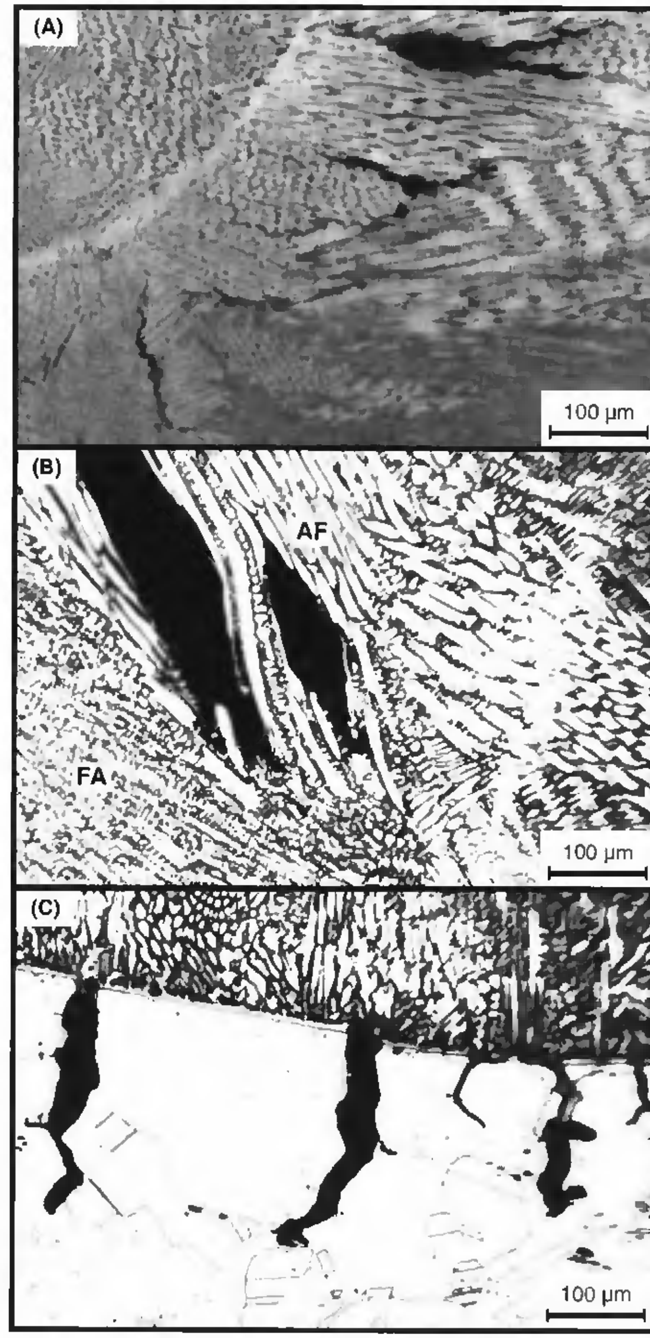

Fig. 3 — Microstructures of type 316L Varestraint specimen tested at 4% strain showing: A — Weld metal cracking; B — a magnified view showing cracking in AF region; and C — base metal HAZ cracking.

Table 3 — Solidification Mode and Ferrite Content of the Weld Metals

			Predicted		Observed	
Material	Cr_{eq}(a)	Ni_{eq}	S. Mode	FN	S. Mode	FN
316L	19.25	12.91	FA	3	FA	2.6
316LN	18.86	13.66	AF	1	AF	0.7
Alloy D9	17.29	17.01	A	0	A	0

(a) WRC-1992 Equivalents: $Cr_{eq} = Cr + Mo + 0.7\ Nb$, $Ni_{eq} = Ni + 35\ C + 20\ N + 0.25\ Cu$

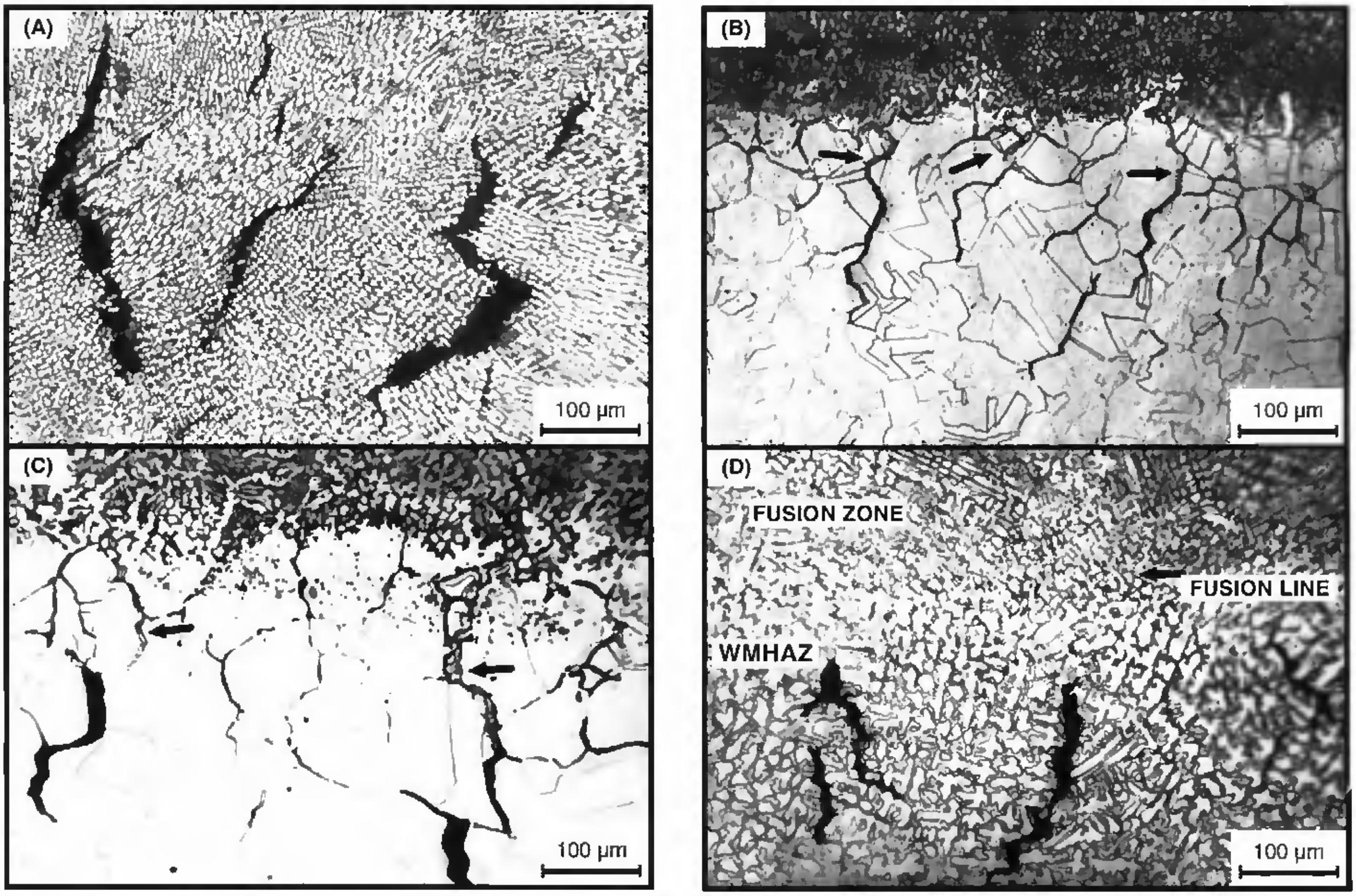

Fig. 4 — Cracking in type 316LN Varestraint specimen tested at 4% strain, showing: A — Weld metal cracking; B — base metal HAZ cracking (arrows indicate backfilling); C — magnified view of backfilling in base metal HAZ crack; and D — weld metal HAZ cracking.

During testing, the strain applied is related to the radius of the die block over which the specimen is bent, by the relation e = t/2R, where e is the strain, t the thickness and R the die block radius. While nominal strain levels of 0.25, 0.5, 1, 2 and 4% were used, the actual strains varied slightly depending on the specimen thickness in each case. Five specimens were tested at each strain level for a given material.

Metallography

After testing, crack lengths were measured on the specimens at 60X using a stereomicroscope. The cracked regions were cut and polished for metallographic observation after crack-length measurements. The polished surfaces were etched electrolytically using either 10% oxalic acid or an aqueous solution of 55% orthophosphoric acid and 12% sulphuric acid. Both light and scanning electron microscopy were used for metallographic examination. The ferrite content of the weld beads was measured using a Magne Gauge calibrated to AWS Standards.

Results

Microstructural Features of Cracking

The as-welded microstructures of the three materials are shown in Fig. 2. The solidification mode of 316L (Fig. 2A) is observed to be mixed, containing both primary ferritic FA regions with vermicular morphology and some primary austenitic AF regions with intercellular ferrite. The 316LN alloy also exhibited a similar structure (Fig. 2B), except that the proportion of AF regions with intercellular ferrite was greater. This indicates that the 316L solidified in the FA/AF mode while the 316LN solidified in the AF/FA mode. The grain boundaries adjoining the weld interface were outlined by retained delta-ferrite, particularly observable in 316LN and much less in 316L. The microstructure of D9 (Fig. 2C) was fully austenitic.

The solidification modes and ferrite contents predicted by the WRC-1992 FN diagram (Ref. 21) for the three materials are shown in Table 3. The ferrite contents measured by Magne Gauge are also tabulated. It is observed that the solidification modes, as well as the ferrite contents predicted, are in agreement with the results obtained by microscopy and magnetic ferrite measurements. However, metallographic observation showed that the ferrite content of 316LN welds was much less in the weld centerline than close to the weld interface.

The microstructures of hot cracks formed in Varestraint specimens tested at 4% strain for the three materials are shown in Figs. 3–5. Figure 3A shows weld metal cracking in 316L exhibiting a mixed ferritic-austenitic solidification mode. The amount of ferrite was 2–3 FN. Cracking was confined to the AF regions and appeared to become arrested when encountering FA regions, as shown in Fig. 3B. Cracks in the BMHAZ were short and wide — Fig. 3C. The cracks were observed to extend up to two or three grains into the BMHAZ. The grain size near the weld interface was large, *i.e.*, about 150 μm grain diameter. Very little cracking was observed in the weld metal HAZ in this material.

The weld metal cracking in Type 316LN is shown in Fig. 4A. The fusion zone showed a large number of cracks,

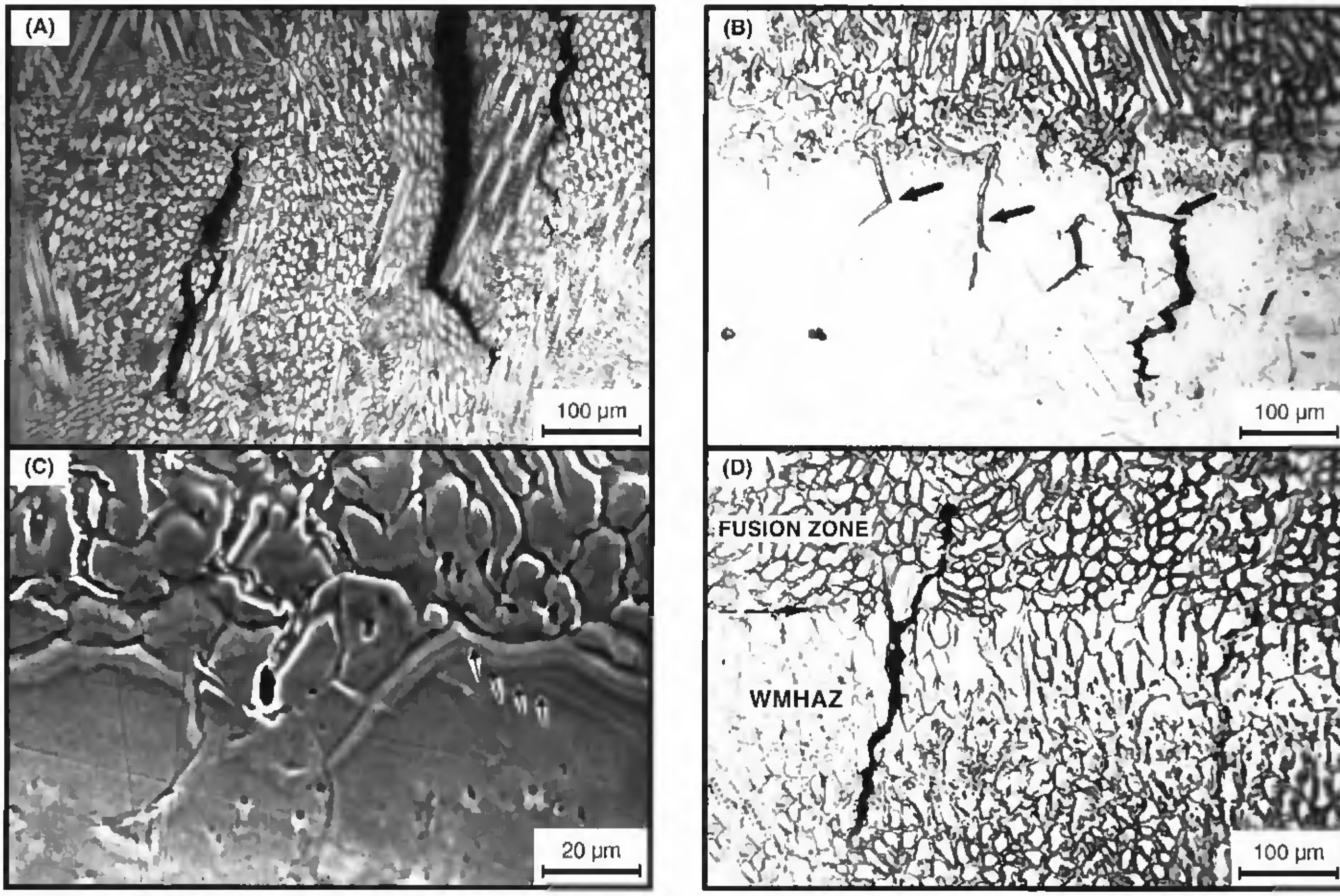

Fig. 5 — Cracking in Alloy D9 Varestraint specimen tested at 4% strain showing: A — Weld metal cracking; B — fully and partially backfilled BMHAZ cracks (indicated by arrows); C — grain boundary migration in the BMHAZ, arrows show successive positions of migrating grain boundary; and D — WMHAZ cracking.

which ranged in size from small microfissures a few microns in length to large ones up to 1 mm long and 50–100 μm wide. Intercellular ferrite was present, though more was present in the 316L weld metal. Unlike in 316L, BMHAZ cracking was extensive, as shown in Figs. 4B and 4C. However, the cracks were extremely fine and narrow in comparison with those in 316L. The grain size in the BMHAZ next to the fusion boundary was also much smaller (50–70 μm). The BMHAZ cracks extended as much as 10 or 12 grains into the base metal. However, as seen in Fig. 4B, most of the cracks were backfilled for 3 or 4 grain widths from the weld interface. Weld metal HAZ cracking occurred to about the same degree as that in the BMHAZ. Some backfilling was also present in the WMHAZ cracks — Fig. 4D.

The fully austenitic Alloy D9 exhibited less cracking in the fusion zone than 316LN. However, a few large, wide cracks were present, as shown in Fig. 5A. BMHAZ cracking was less than that in 316L or 316LN. As in 316LN, backfilling was present in many cracks. Cracks extended along only a few of the liquated grains, although liquation of grain boundaries could be observed all along the weld interface. These observations are illustrated in Figs. 5B and 5C, which show optical and SEM photomicrographs of the same region. Unlike in the other two materials, the liquated boundaries were much wider in D9 and were therefore more clearly visible even at low magnifications. Figure 5C shows an SEM micrograph where the liquated grain boundaries have migrated. The liquation and subsequent resolidification of the boundary has produced a segregation pattern at three or four positions, presumably due to pinning by solutes or fine precipitates during the weld thermal cycle. Such "ghost boundaries" were absent in the other two materials. Weld metal HAZ cracking was quite insignificant in D9, although a few isolated cracks were present, as shown in Fig. 5D.

Crack Length Measurements

The results of crack length measurements carried out on a stereomicroscope at 60X are shown in Figs. 6–10. The total crack length (TCL) in the fusion zone is shown as a function of strain level in Fig. 6. Type 316L showed good cracking resistance as the TCL was below 0.5 mm up to 2% strain, increasing to slightly above 2.5 mm only at 4% strain. On the other hand, 316LN showed significant cracking (1.5 mm) even at the smallest strain of 0.25%, which increased to a high value of 8.5 mm at 4% strain. D9 exhibited a cracking tendency intermediate between those of 316L and 316LN, the TCL values increasing from 2 mm at 1% strain to 5.75 mm at 4% strain.

Cracking in the base metal HAZ is shown in Fig. 7, where it is observed that all three materials exhibit cracking only above a threshold of 1% strain. At 4% strain, the 316L has a higher TCL than either D9 or 316LN, although at 2% strain the TCL values in 316LN and 316L are nearly equal. Note this observation is in divergence with the metallographic observation of cracking on polished and etched specimens. In the WMHAZ (Fig. 8), 316LN exhibiting a TCL of nearly 1 mm was far more susceptible than the other two materials, which appeared to be resistant to this type of cracking. Cracking occurred only beyond a threshold strain of 2% in 316L and Alloy D9.

The maximum crack length values in the fusion zone are shown as a function of strain level in Fig. 9. The maximum crack length sharply increases with strain for Type 316LN and D9, unlike 316L, where it remains quite low, *i.e.*, at about 0.1 mm up to 2% strain. Also, the curves for 316LN and D9 show a clear separation from that of the 316L.

Appreciable backfilling was present in the HAZ cracks of 316LN and D9. To evaluate the backfilling, specimens were polished, etched and viewed at 180X. The results of the observations are shown in Fig. 10. No weld metal HAZ cracking was observed in 316L. Backfilling was present in the weld metal and HAZ of all three materials. However, the extent of backfilling was greater in HAZ cracks of 316LN and in D9, as shown in Fig. 10. The backfilled crack length is nearly 50% of the total crack length in 316LN and D9, while it is only 10–15% in 316L.

It is also evident from Fig. 10 that the cracking is actually greater in 316LN than in 316L. This data is supported by the metallographic observations of BMHAZ cracking (Figs. 3B and 4B), which show a few large cracks in 316L, while a large number of very fine cracks were present in the 316L. The results shown in Fig. 10 apparently contradict those shown in Fig. 7. The data in Fig. 7 were obtained on as-welded specimens where the cracking was measured at 60X using a stereomicroscope, whereas the data in Fig. 10 were obtained from polished and etched sections at 180X. This suggests that the estimation of HAZ cracks in Varestraint Test specimens at low magnifications can be misleading, as fine cracks may escape detection.

Discussion

Use of Varestraint Evaluation Criteria in Cracking Assessment

In the present work, alloy 316L solidified in the FA/AF mode and 316LN in the AF/FA mode, while D9 was fully austenitic. Using the TCL criterion, the 316LN shows the highest susceptibility to cracking, followed by D9 and 316L. However, by the MCL criteria, there is very little difference between 316LN and D9. The 316L exhibits a low cracking tendency by both criteria. According to Lundin, *et al.* (Ref. 22), the TCL and cracking threshold criteria taken together give the best assessment of material weldability. However, several workers have also used the MCL to describe material weldability (Refs.12, 23).

The present results show that the 316LN specimens cracked much more than D9 in the fusion zone, as shown metallographically in Figs. 4A and 5A. While both 316LN and D9 have austenite as the primary solidifying phase and exhibit nearly the same MCL, the level of impurity elements is much less in D9 (0.014% P+S) than in 316LN (0.033%). It appears the MCL values are sensitive to

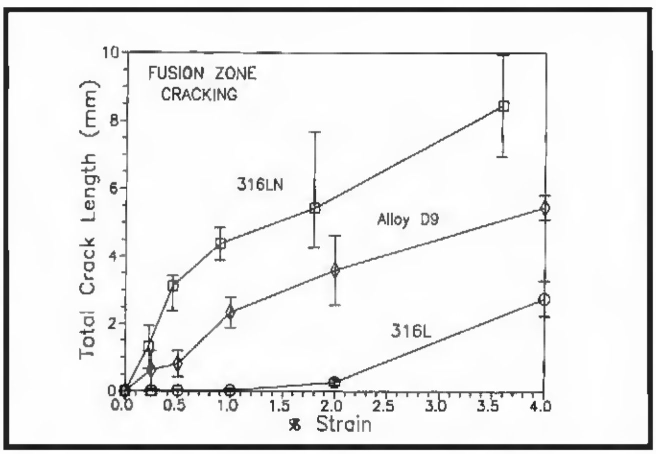

Fig. 6 — Total fusion zone crack length as a function of strain applied during Varestraint testing.

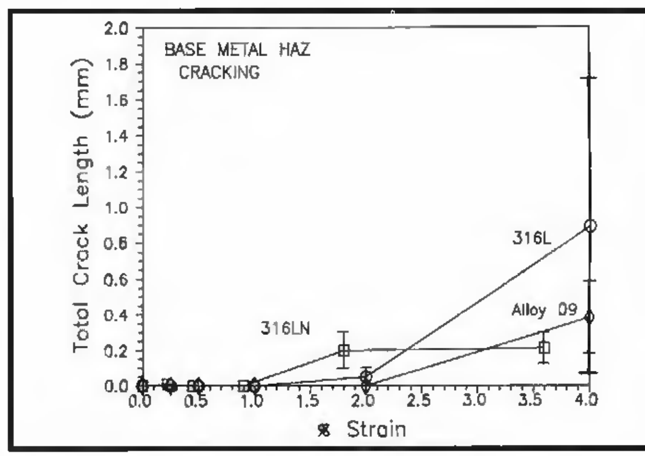

Fig. 7 — Total crack length in the base metal HAZ as a function of strain applied during Varestraint testing.

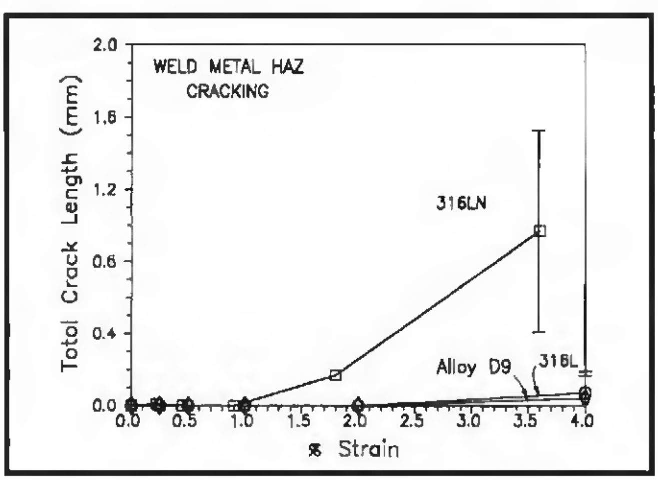

Fig. 8 — Variation of total crack length in the WMHAZ with strain applied during Varestraint testing.

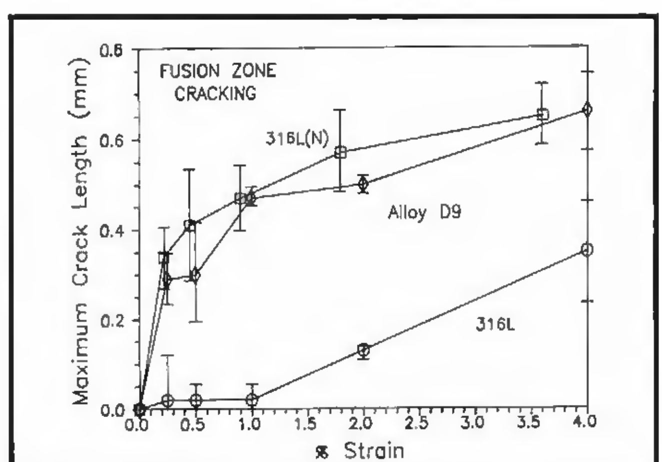

Fig. 9 — Maximum crack length as a function of strain applied during Varestraint testing.

the solidification mode but not to relatively minor variations in impurity element levels. The distinction in weldability between the materials is clear only through the TCL data. Hence, our results show that the TCL criterion is a better measure of weldability than the MCL evaluated using the longitudinal Varestraint Test.

Influence of Primary Solidification Mode and Impurity Content on Cracking Behavior

It is observed from Table 3 that the solidification modes and ferrite potentials of the three materials have been predicted accurately by the WRC-1992 FN diagram. Since weld solidification cracking in stainless steels is a function of solidification mode, ferrite content and impurity element levels, the results of hot cracking tests have often been represented on a map of chromium equivalent to nickel equivalent ratio (Cr_{eq}/Ni_{eq}) vs. P+S content (Ref. 6). In Fig. 11, a modified version due to Lundin (Ref. 14) is used where a regime is included for the occurrence of a mixed solidification mode. Compositions of various Type 304 and 316 alloys in the literature have been plotted on this diagram, along with hot cracking results (Refs. 4, 12, 14, 24). On this diagram, the elements having a high Cr_{eq}/Ni_{eq} ratio and, consequently, an FA/F solidification mode, would be relatively insensitive to impurity levels, *i.e.*, the total crack length as determined by the Varestraint Test at 4% strain level would be less than 1.5 mm. The observed behavior of the 316L and D9 materials is consistent with their positions on this diagram. On the other hand, 316LN is much more sensitive to cracking than its location would suggest. With a P+S content of 0.032%, a total crack length of 8.5 mm is observed at 4% strain. Matsuda, *et al.* (Ref. 12), observed that the addition of nitrogen aggravated the segregation of phosphorus leading to an increase in the brittleness temperature range to levels obtained in fully austenitic materials. The data of Matsuda, *et al.*, have been shown in Fig. 11, where it is seen that an increase in nitrogen content from 0.02 to 0.09% increased the BTR in Type 304-A weld metal (0.03% P, 0.005% S) from 60 K to 140 K, indicating high susceptibility. The corresponding change in Cr_{eq}/Ni_{eq}, however, brings the composition only to the edge of the "susceptible" range — Fig. 11. A further increase in the nitrogen level to 0.15% marginally increased BTR from 140 to 150 K. In 304-B weld metal, where the P content was slightly less (0.026% P, 0.005% S), the BTR only increased from 50 to 80 K with a corre-

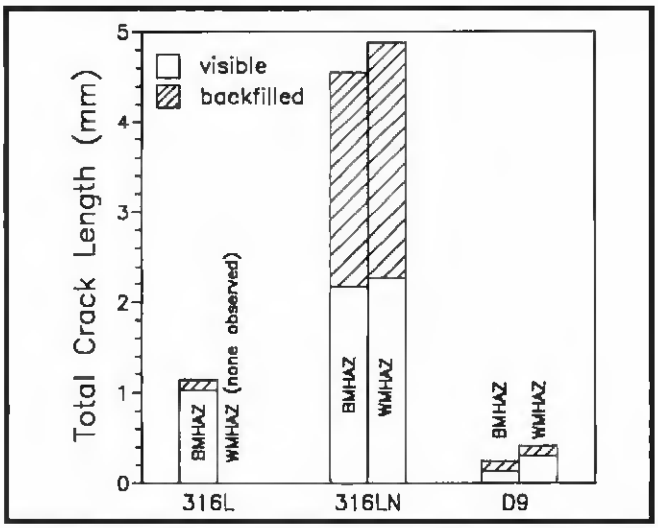

Fig. 10 — The extent of backfilling in HAZ cracks of specimens tested at 4% strain.

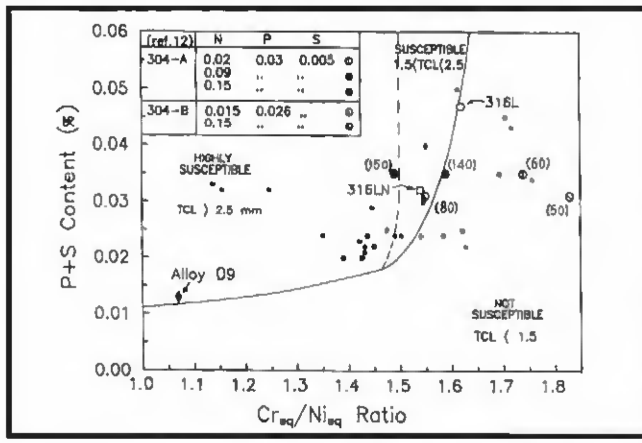

Fig. 11 — Hot cracking susceptibility of Type 316 and 304 materials as a function of Cr_{eq}/Ni_{eq} ratio and P+S content. The data shown are from Refs. 4, 11, 13 and 22 along with the present work. The figures in parentheses represent BTR (K). Fully shaded points indicate high susceptibility. (Cr_{eq} = Cr + 1.37Mo + 1.5Si + 2Nb + 3Ti and Ni_{eq} = Ni + 0.31Mn + 22C + 14.2N + Cu).

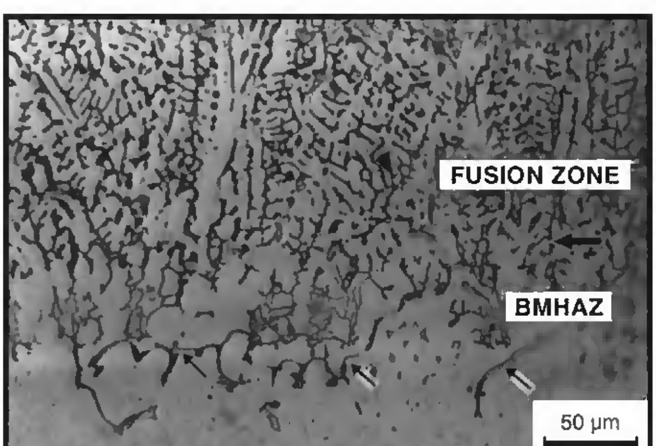

Fig. 12 — Weld interface microstructure of type 316LN weld showing extensive δ-ferrite formation in the HAZ grain interiors and grain boundaries. Grain boundaries showing liquation are marked by arrows.

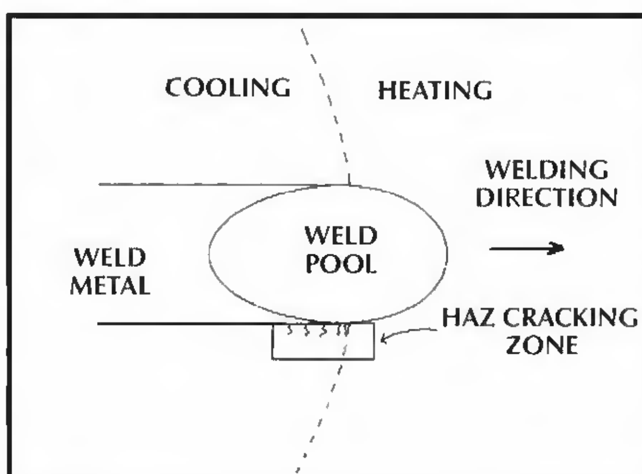

Fig. 13 — The relationship between weld thermal zones and the location of HAZ cracking.

sponding change from the "not susceptible" to the "susceptible" region. This indicates that the susceptibility is dependent on the level of phosphorus in addition to that of nitrogen. The present results and those of Matsuda, *et al.*, show that there is some evidence of an interaction between P and N in increasing cracking. It is also evident that the map of Cr_{eq}/Ni_{eq} ratio vs. (P+S) content may only provide a clear indication of cracking susceptibility between widely different compositions. The diagram cannot be relied upon to predict cracking susceptibility in the critical regime of Cr_{eq}/Ni_{eq} = 1.5–1.6, where a small change in composition could result in a large change in susceptibility.

Microstructural Features of HAZ Cracking

The HAZ cracking presented several interesting microstructural features such as delta-ferrite formation, backfilling of cracks and segregation effects. Backfilling of HAZ cracks occurred in 316LN and D9, in which the HAZ grain boundaries exhibited extensive liquation — Figs. 4B, 5B and 5C. Additionally, "ghost boundaries," as reported earlier by Lippold in Alloy 800 (Ref. 17), were found in the BMHAZ of D9. The formation of such boundaries has been attributed to the "sweeping" or pickup of solutes by grain boundaries migrating under the action of thermal and shrinkage stresses (Refs. 25, 26). The boundaries become visible as a result of solute enrichment at positions where the rapid movement of the grain boundary leaves behind solute atoms, which were unable to diffuse with the migrating grain boundary. Such boundaries may liquate when the concentration of solute atoms produces constitutional liquation (Ref. 25). Further, Alloy D9 contains 0.33%Ti, which was one of the elements identified by Lippold (Ref. 17) in liquated grain boundaries of Alloy 800 and A286.

Effect of Delta-Ferrite on HAZ Cracking

The BMHAZ grain boundaries at the weld interface exhibited delta-ferrite in 316L and 316LN. However, in 316LN, even the grain interiors were observed to be decorated by retained delta-ferrite with a lacy morphology (Fig. 12), which is unusual in a material with a low ferrite potential of 1 FN. Lacy or lathy ferrite occurs when the ferrite formed during the heating cycle partially retransforms to austenite at much lower temperatures. The lower temperature of transformation favors an orientation relationship between delta-ferrite and austenite, and results in a lathy morphology of ferrite (Ref. 27). In conventional type 316L, the retained delta-ferrite has been found to grow with increasing ferrite potential. However, in the present case, the 316LN contains 0.073% N, which can have a significant influence on the formation and retransformation of delta-ferrite in the HAZ. The effect of nitrogen on the austenite-ferrite transformation has not been clearly understood.

The formation of δ-ferrite at grain boundaries has been found to retard cracking in the HAZ (Ref. 28). Lippold, *et al.* (Ref. 29), have shown that materials with a high ferrite potential in the HAZ are resistant to HAZ cracking. The present results confirm this, since higher ferrite potential 316L exhibited lower cracking than 316LN — Fig. 10. In 316LN, the cracking extended for 7–8 grains into the BMHAZ, where δ-ferrite was not observed. However, close to the weld interface where δ-ferrite formation occurred, most of the cracks were backfilled for 3–4 grain-widths. Delta-ferrite was also observed in some of the backfilled regions — Fig. 4C. However, these features cannot be taken to imply that the presence of δ-ferrite in the grain boundary inhibited the original cracking since the backfilled region could contain liquid with a different composition than that of the base metal.

In the weld metal HAZ, extensive cracking was observed in 316LN — Fig. 8. Lundin and Chou (Ref. 30) found that dissolution of the delta-ferrite in the underlying weld bead could lead to enhanced cracking. They postulated that when the ferrite content of this "hazard HAZ" was below 1 FN, the dissolution of the ferrite released the impurity elements present in it to the austenite, which caused cracking by interfacial segregation. In a subsequent study, it was found (Ref. 15) that the number of fissures in the Fissure Bend Test increased in FA materials with increasing nitrogen concentration. The tendency of N to aggravate P segregation was referred to earlier. The high degree of HAZ cracking observed in 316LN with N = 0.073 & P = 0.031% could thus be a result of an interactive effect between N & P.

Backfilling of HAZ Cracks

Backfilling of HAZ cracks has been previously observed in high-alloy stainless steels Alloy 800 (Ref. 17), A286 (Ref. 29), high-nickel alloys Incoloy 903 and 909 and Alloy 718 (Ref. 31). In 316LN and Alloy D9, the HAZ liquation cracks have presumably initiated at the weld interface grain boundaries, which show signs of extensive liquation, and propagated into the HAZ. Such propagation has occurred several grains deep, and, as observed in the micrographs (Figs. 4B and 4C), there is no sign of liquation visible at the tip of the cracks. It is not clear how the HAZ cracks grow beyond the region where extensive liquation is observable, although several explanations including liquid metal embrittlement have been offered by Lippold, *et al.* (Ref. 29). The grain boundaries may be backfilled as much as 200 μm into the HAZ (Fig. 4C), although this is related to the general tendency for HAZ cracking.

The backfilling of solidification cracks has been investigated in detail by Lundin, *et al.* (Ref. 32). They found that the extent of backfilling was a function of thermal conditions, composition and capillary dimension. Thus, the weld centerline where thermal gradient was lowest, an FA solidification mode and narrow cracks favored backfilling. In the present work, backfilling was observed to a significant extent in the HAZ cracks of 316LN and D9 materials (Fig. 10). We find that the portion of the HAZ in a weld bead where cracking occurs is located at the intersection of the heating and cooling fronts that result from the movement of the welding arc. This is illustrated in Fig. 13, in which the thermal zones associated with the weld pool during welding are shown (Refs. 33, 34). The points near the weld interface experience the highest temperature in the HAZ in the solid state. When compared with the weld centerline, these points experience high temperatures in the solid state for a longer period of time, which can be inferred by considering the thermal cycles for the two points. Moreover, the solidification rate R is nearly zero at this location (Ref. 34), which increases the availability of the liquid for backfilling to occur. Hence, if capillary conditions are favorable, backfilling should easily occur in the HAZ cracks.

The relationship between the composition and the extent of backfilling in the case of HAZ cracking is less clear than in the weld metal. Of the three compositions investigated, 316LN and D9 exhibited backfilling, which was not observed to any significant extent in 316L. Backfilling should be easier if the liquid being drawn into the crack possesses a lower melting point and easily wets the grain boundaries. Since austenite-austenite grain boundaries are more easily wetted than austenite-ferrite boundaries, backfilling should be easier in low ferrite potential materials, if other conditions are favorable. The appreciable backfilling observed in D9 alloy illustrates this point (Fig. 5B and Fig. 10). Moreover, small changes in impurity and minor element levels could change the wetting characteristics of the remaining liquid. Thus, both solidification mode and impurity element levels may affect backfilling in a complex way. Since the grain size in the HAZ of 316L was coarser than in 316LN, the cracks were wider and less prone to backfilling, whereas the narrow cracks in the latter were extensively backfilled. However, in the WMHAZ, the interdendritic spacing of the underlying weld metal would influence both cracking as well as backfilling. Segregation is already present in the WMHAZ and the lowest melting constituents are available in the interdendritic regions. This might increase the wettability of WMHAZ cracks and make them more liable for backfilling than the BMHAZ cracks. Lippold, *et al.* (Ref. 29), did not observe the extensive backfilling in 304L and 316L compositions similar to those of this study. However, they used the spot Varestraint Test procedure, where the thermal conditions are different from that in the moving torch test, producing a significant difference in backfilling of the HAZ cracks.

Conclusions

Hot cracking in nitrogen-bearing 316LN stainless steel and fully austenitic D9 alloy was compared with that in a conventional Type 316L composition. The following conclusions were obtained from this study:

1) The nitrogen-bearing 316LN alloy was highly susceptible to cracking in the weld metal and in the HAZ. The extent of cracking was greater than that could be ascribed to the AF solidification mode, ferrite potential and impurity element concentration in this alloy.

2) Cracking in D9 alloy conformed to that of fully austenitic materials and exhibited features typical of Ti-stabilized austenitic alloys.

3) The HAZ in the 316LN and D9 alloys was prone to backfilling. Backfilling was favored in the HAZ cracks because of a favorable thermal field; it is also facilitated by capillary conditions, especially in fine-grained base metal.

Acknowledgments

The authors thank Dr. Placid Rodriguez, Director, IGCAR and Dr. Baldev Raj, Director, MMG for their encouragement and keen interest in this work. The assistance of G. Srinivasan and Ram Mohan during experimentation is gratefully acknowledged.

References

1. Apblett, W. R., and Pellini, W. S. 1954. Factors which influence weld hot cracking. *Welding Journal* 33(2): 83-s to 90-s.

2. Borland, J. C. 1960. Generalized theory of super-solidus cracking in welds (and castings). *British Welding Journal* 7(8): 508–512.

3. Hull, F. C. 1960. Effects of alloying additions on hot cracking of austenitic stainless steels. *Trans. ASTM* 60: 667–690.

4. Lundin, C. D., DeLong, W. T., and Spond, D. F. 1975. Ferrite-fissuring relationships in austenitic stainless steel weld metals. *Welding Journal* 54(7): 241-s to 246-s.

5. Masumoto, I., Takami, K., and Kutsuna, M. 1972. Hot cracking of austenitic stainless steel weld metal. *Journal of the JWS* 41(11): 1306–1314.

6. Kujanpaa, V., Suutala, N., Takalo, T., and Moisio, T. 1979. Correlation between solidification cracking and microstructure in austenitic and austenitic-ferritic stainless steel welds. *Journal of Welding Research International* 9(2): 55–75.

7. Arata, Y., Matsuda, F., Nakagawa, H., and Katayama, S. 1978. Solidification crack susceptibility in weld metals of fully austenitic stainless steels (Report IV) — effect of decreasing P and S on solidification crack susceptibility of SUS 310 weld metals. *Trans. Jap. Weld. Res. Inst.* 7(2): 169–172.

8. Maziasz, P. J. 1989. Developing an austenitic stainless steel for improved performance in advanced fossil power facilities. *J. of Metals* (12): 14–20.

9. Ogawa, T., and Tsunetomi, E. 1982. Hot cracking susceptibility of austenitic stainless steels. *Welding Journal* 61(3): 82-s to 93-s.

10. Okagawa, R. K., Dixon, R. D., and Olson, D. L. 1983. The influence of nitrogen from welding on stainless steel weld microstructures. *Welding Journal* 62(8): 204-s to 209-s.

11. Olson, D. L. 1985. Prediction of austenitic weld metal microstructure and properties. *Welding Journal* 64(10): 281-s to 295-s.

12. Matsuda, F., Nakagawa, H., Katayama, S., and Arata, Y. 1983. Solidification crack susceptibility in weld metals of fully austenitic stainless steels (Report VIII) — Effect of nitrogen on cracking in SUS 304 weld metal. *Trans. JWRI* 12(1): 89–95.

13. Ogawa, T., Suzuki, K., and Zaizen, T. 1984. The weldability of nitrogen-containing austenitic stainless steel: Part II — porosity, cracking and creep properties. *Welding Journal* 63(7): 213-s to 223-s.

14. Lundin, C. D., Lee, C. H., and Qiao, C. Y. P. 1988. Group sponsored study—weldability and hot ductility behavior of nuclear grade austenitic stainless steels. *Final Report*, Univ. of Tennessee, Knoxville, Tenn.

15. Lundin, C. D., and Chou, C-P. D. 1985. Fissuring in the "hazard HAZ" region of austenitic stainless steel welds. *Welding Journal* 64(4): 113-s to 118-s.

16. Chou, C. -P. D., and Wu, P. -S. 1986. Effect of nitrogen on the austenitic stainless steel weld metal HAZ cracking. *Advances in Welding Science and Technology*, ed. S. A. David, ASM, 703–707.

17. Lippold, J. C. 1983. An investigation of heat-affected zone hot cracking in Alloy 800. *Welding Journal* 62(1): 1-s to 11-s.

18. Brooks, J. A. 1974. Effect of alloy modifications on HAZ cracking of A-286 stainless steel. *Welding Journal* 53(11): 517-s to 523-s.

19. Lundin, C. D., Menon, R., Lee, C. H., and Osorio, V. 1985. New concepts in Varestraint testing for hot cracking. *Welding Research: The State of the Art*. JDC University Research Symposium Proceedings, ASM.

20. Lundin, C. D., Lee, C. H., Menon, R., and Osorio, V. 1988. Weldability evaluations of modified 316 and 347 austenitic stainless steels: Part I — preliminary results. *Welding Journal* 67(2): 35-s to 46-s.

21. Kotecki, D. J., and Siewert, T.A. 1992. WRC-1992 constitution diagram for stainless steel weld metals: a modification of the WRC-1988 diagram. *Welding Journal* 71(5): 171-s to 178-s.

22. Lundin, C. D., Lingenfelter, A. C., Grotke, G. E., Lessman, G. G., and Mathews, S. J. 1982. The Varestraint Test. *WRC Bulletin No. 280*. Welding Research Council, New York.

23. Arata, Y., Matsuda, F., and Katayama, S. 1977. Solidification crack susceptibility in weld metals of fully austenitic stainless steels (Report II) — effect of ferrite, P, S, C, Si and Mn on ductility properties of solidification brittleness. *Trans. JWRI* 6(1): 105–116.

24. Gooch, T. G., and Honeycombe, J. 1980. Welding variables and microfissuring in austenitic stainless steel weld metal. *Welding Journal* 59(8): 233-s to 241-s.

25. Pepe, J. J., and Savage, W. F. 1967. Effects of constitutional liquation on 18-Ni maraging steel weldments. *Welding Journal* 46(9): 411-s to 422-s.

26. Pepe, J. J., and Savage, W. F. 1970. The weld heat-affected zone of the 18-Ni maraging steels. *Welding Journal* 49(12): 545-s.

27. Brooks, J. A., and Thompson, A.W. 1991. Microstructural development and solidification cracking susceptibility of austenitic stainless steel welds. *Int. Mater. Rev.* 36(1): 16–44.

28. Kujanpaa, V. P., David, S. A., and White, C. L. 1987. Characterization of heat-affected zone cracking in austenitic stainless steel welds. *Welding Journal* 66(8): 221-s to 228-s.

29. Lippold, J. C., Baeslak III, W. A., and Varol, I. 1992. Heat-affected zone liquation cracking in austenitic and duplex stainless steels. *Welding Journal*. 71(1): 1-s to 14-s.

30. Lundin, C. D., and Chou, C.-P.D. 1983. Hot cracking of austenitic stainless steel weld metals. *WRC Bulletin No. 289*. Welding Research Council, New York.

31. Thompson, R. G., and Genculu, S. 1983. Microstructural evolution in the HAZ of Inconel 718 and correlation with the hot ductility test. *Welding Journal*. 62(12): 377-s.

32. Lundin, C. D., Lee, C. H., and Quao, C. Y. P. 1993. Evaluation of backfilled solidification cracks in austenitic stainless welds in relationship to evaluation of hot cracking. *Welding Journal* 72(7): 321-s to 328-s.

33. Rosenthal, D. 1946. The theory of moving sources of heat and its application to metal treatments. *Trans. ASME* 68: 849–866.

34. David, S. A., and Vitek, J. M. 1989. Correlation between solidification parameters and weld microstructures. *Int. Mater. Rev.* 34(5): 213–245.